State to State to State Dynamics of the $D + H_2 \rightarrow HD + H$ Reaction: Control of Transition-State Pathways via Reagent Orientation

Jianyang Zhang,[1] Dongxu Dai,[1] Chia C. Wang,[1] Steven A. Harich,[1] Xiuyan Wang,[1] Xueming Yang,[1,*] Magnus Gustafsson,[2] and Rex T. Skodje[2,*]

[1]*Dalian Institute of Chemical Physics, Chinese Academy of Sciences, Dalian, China*
[2]*Institute of Atomic and Molecular Sciences, Academia Sinica, P.O. Box 23-166, Taipei, Taiwan and Department of Chemistry and Biochemistry, University of Colorado, Boulder, Colorado 80309, USA*

(Received 8 September 2005; revised manuscript received 22 February 2006; published 9 March 2006)

The influence of reagent rotation on the dynamics of the $D + H_2 \rightarrow HD + H$ reaction is studied. The state-resolved differential cross section is measured using the Rydberg-atom scheme in a crossed beam experiment. It is found that the H_2 rotation has a strong influence on the results. This effect was traced to the selection of the quantum bottleneck states through reagent orientation, thus suggesting a novel strategy to control the transition-state pathways in direct chemical reactions.

DOI: 10.1103/PhysRevLett.96.093201 PACS numbers: 34.50.Lf

One of the most interesting issues under current study in the field of molecular dynamics is the influence of reagent rotation on the outcome of chemical reactions [1]. While quantum scattering theory can be used to generate the initial state selected differential cross section (DCS), the elaborate computations tend to obscure the physical picture of the underlying dynamics. Therefore, fundamental questions remain unanswered, such as how the rotational state and alignment affect the passage through the transition state (TS) of the reaction. Furthermore, it is unclear precisely how the details of this TS dynamics influence the state and angle product distribution, which are the observables in a collision experiment.

The notion that the properties of the transition state are imprinted on the detailed observables of a reactive collision is a piece of conventional wisdom. The ''Polanyi rules'' [2] relating the location of the TS to the role of vibrational excitation of either reagents or products provides a well-known early example. More recently, the relationship of the bending dynamics at the TS to the rotational product distribution has been investigated for a number of bimolecular [3,4] and unimolecular reactions [5,6]. The control of reactivity by quantized bottleneck states (QBS) has been suggested by Truhlar and coworkers [7,8]. The QBS, which refer to unbound Seigert states [9] localized near the barriers of vibrationally adiabatic potentials, provide a rigorous representation of the internal excitation of the collision complex near the TS. Recently, it was demonstrated that unmistakable signatures of QBS appear in the DCS of reactions $D + HD$ and $H + D_2$ [10–13]. However, it remains unclear what is the precise role of rotational orientation of the reagents within this picture.

In this Letter, we present results of a new molecular beam experiment and of theoretical dynamics calculations for the $D + H_2 \rightarrow HD + H$ reaction. The influence of reagent rotation on the reaction is probed by comparing the results obtained from the para (p) and ortho (o) forms of H_2, which correlate uniquely to the $H_2(j = 0)$ and $H_2(j = 1)$ states. The reaction process is found to proceed through well-defined quantum pathways at the TS that are strongly correlated by symmetry to the orientation of the reagent molecules.

We investigate the dynamics of the $D + H_2 \rightarrow HD(v', j') + H$ reaction using a crossed molecular beam apparatus. Two parallel molecular beams (DI and H_2) are generated with pulsed valves. The D-atom beam is produced by DI photolysis using the fourth harmonic of a YAG laser or a KrF laser. The H_2 beam (either p-H_2 or n-H_2) was produced by an adiabatic expansion through a nozzle cooled by liquid nitrogen. The p-H_2 beam, produced by flowing n-H_2 through the cryogenically cooled o-p conversion catalysis, was almost all in the $j = 0$ state, while n-H_2 beam consisted of $j = 0(p)$ and $j = 1(o)$ states in a ratio of 1:3. The beam densities for both forms of H_2 were kept equal and the reactive scattering signal for the o-$H_2(j = 1)$ reagent was found by combining the signals from p-H_2 and n-H_2 reactions. The reaction was studied for the center-of-mass collision energies $E_C = 0.315$, 0.484, 0.783, and 0.945 eV with a thermal spread of about $\Delta E_C = 10$ meV. The reaction products were monitored using the H atom Rydberg time-of-flight (TOF) technique [14]. The TOF spectra of product H atoms were measured and assigned to HD-product rovibrational states, which then yield the relative quantum state-specific DCS with typical errors less than $\pm 10\%$. The relative DCS of $D + p$-H_2 and $D + o$-H_2 are well defined without the need for a scaling factor.

The backward scattering DCS versus j' is shown in Fig. 1. Near the reaction threshold, $E_C = 0.315$ eV, the distribution of product states is unimodal and centered near $HD(j' = 2)$. The signal for the o-H_2 reagent is noticeably higher than that for p-H_2. At the higher collision energy, $E_C = 0.783$ eV, the product state distributions have shifted significantly. The p-H_2 reagent yields a bimodal distribution peaked at $j' = 3$ and $j' = 8$. The o-H_2 reagent

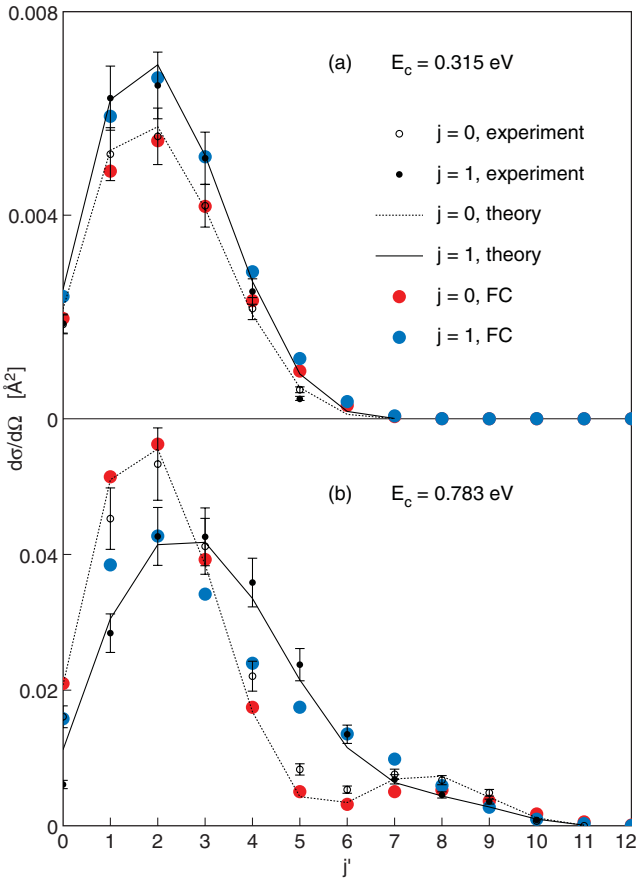

FIG. 1 (color). The rotational product state distribution for $D + H_2 \rightarrow HD(v' = 0, j') + H$ obtained at the LAB angle of ~95° ($\theta_{CM} \sim 175°$). The experimental, exact scattering (theory), and FC-treatment of the state-to-state-to-state model are compared at two collision energies.

gives a distribution that is clearly different from the p-H_2 result with the bimodal character suppressed. The bimodal character of the distribution, and the difference between p-H_2 and o-H_2, becomes more pronounced at higher E_C. The strong distinction between the reactivity of p-H_2 and o-H_2 was unexpected, [15] and at this point, unexplained by a dynamical mechanism.

A theoretical simulation of the $D + H_2$ reaction was carried out using a fully converged coupled-channel scattering calculation that employed the accurate BKMP2-PES [16]. The S matrix is produced from a coupled-channel calculation in a hyperspherical coordinate system [17,18] using a partial wave expansion up to total angular momentum $J = 38$ on a grid of 110 total energies from $E =$ 0.3–1.6 eV. In Fig. 1, we see that the theoretical model accurately reproduces the product state distributions seen experimentally. Even though the simulation does not "explain" the result, it does indicate that the model is adequate for use in a more detailed analysis.

The distinction between the reactivity of p-H_2 and o-H_2 molecules is quite fascinating since it probes the influence of reagent rotation on reaction. The small para-ortho energy splitting cannot explain the differences that actually grow more pronounced with larger E_C. Instead, the p-H_2 and o-H_2 appear to cross the TS differently in a manner controlled by the orientation of H_2. While the p-$H_2(j = 0)$ beam lies in the $k = 0$ helicity state, the o-$H_2(j = 1)$ beam is composed of 2/3 "helicopter" rotation ($k = \pm 1$) and 1/3 "cartwheel" rotation ($k = 0$). Since the reaction path is collinear for $D + H_2$, the QBS are labeled by the quantum numbers for a linear triatom, $\boldsymbol{n} \equiv (\nu_{\text{sym-str}}, \nu^{\Lambda}_{\text{bend}})$, where the reaction coordinate is frozen. We find k correlates most strongly to the QBS vibrational-angular momentum, Λ. Schatz and Kuppermann [19] have noted that the helicity is exactly conserved, $k = k'$, along the CM (forward-backward) collision axis, and at nearby angles the helicity conserving approximation is often accurate. Extending this scattering result to the intermediate TS region, we have $k \approx \Lambda \approx k'$. This implies that only those QBS with $\Lambda = 0$ contribute to the $D + p$-H_2 reaction since $k = 0$. For $D + o$-H_2, on the other hand, QBS with $\Lambda = 0, \pm 1$ can all contribute since $k = 0$ or ± 1. Therefore, the $k = 0$ reagent molecules must pass through the QBS with $\nu^{\Lambda}_{\text{bend}} = 0^0, 2^0, \ldots$, while the $k = \pm 1$ states must cross the TS through the $\nu^{\Lambda}_{\text{bend}} = 1^{\pm 1}, 3^{\pm 1}, \ldots$ states. The differences between p-H_2 and o-H_2 reactivity arises from these distinct pathways through the TS.

To elucidate this idea, consider first the total reaction probabilities (P_R) computed for the $k = 0$ and $k = \pm 1$ states of o-H_2. As seen in Fig. 2(a), the threshold in P_R for $D + o$-$H_2(k = \pm 1)$ is 100 meV higher than for $D + o$-$H_2(k = 0)$. The threshold for the $D + o$-$H_2(k = 0)$ reaction is consistent with the passage through the lowest lying $\Lambda = 0$ QBS, $(0, 0^0)$, that lies at $E_C = 0.35$ eV. On the other hand, the threshold for $D + o$-$H_2(k = \pm 1)$ is consistent with passage through the lowest lying $\Lambda = \pm 1$ state, $(0, 1^{\pm})$, that lies at 0.45 eV. Furthermore, we have used the exact energy and width of these two QBS's to construct a one-dimensional barrier transmission probability (see below), which is in excellent agreement with the exact quantum mechanical calculations as shown in Fig. 2(a). The $D + p$-H_2 reaction exhibits nearly identical threshold behavior to $D + o$-$H_2(k = 0)$. While the result $k = \Lambda = k'$ does not hold exactly for P_R, the present calculations demonstrate that it is an excellent approximation for low impact parameters. Indeed, as illustrated in Fig. 2(b), this threshold behavior survives the impact parameter average and carries over to the DCS. Clearly, the threshold for the helicity states is completely controlled by QBS of different symmetries. The implication of this result is exciting since the control of TS pathways via reagent helicity selection has proven feasible.

In the state-to-state-to-state model, we view a direct chemical reaction as a coherent three-step process. The incoming reagent flux is scrambled by coupling in the entrance channel to populate a number of energetically

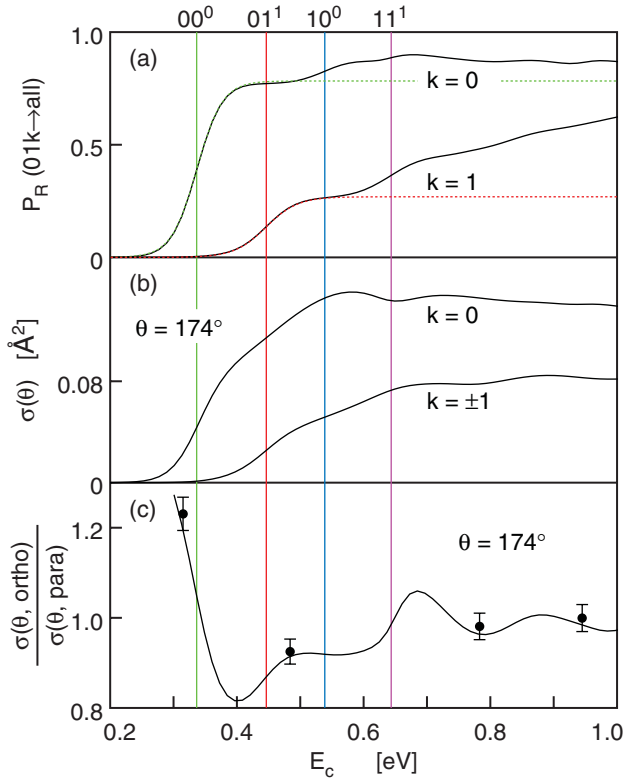

FIG. 2 (color). A comparison of reaction attributes for the p-H_2 and o-H_2 reagent. In (a), the exact quantum scattering P_R is plotted vs E_C for the $k = 0$ and $k = \pm 1$ states of $D + o$-H_2. The dashed lines are the model prediction employing, for clarity, only the lowest symmetry allowed QBS. The energies of the bend progression of QBS are shown with vertical lines. In (b), the total reactive DCS at $\theta_{\mathrm{LAB}} \approx 95°$ for the $k = 0$ and $k = \pm 1$ states of o-H_2 are plotted. In (c), we show the ratio of total backward DCS for $D + o$-H_2 and $D + p$-H_2.

allowed QBS. The passage through the TS region is assumed separable in the QBS basis (the nonrecrossing hypothesis of transition state theory (TST). In the exit channel, the coupling again scrambles the flux thus giving rise to interfering reactive pathways through the TS. This analog of TST for state-to-state chemistry is described by the factorized S matrix [12] $\mathbf{S}(E) = \mathbf{S}_0^- \cdot \mathbf{S}_{na}^- \cdot \mathbf{S}_b \cdot \mathbf{S}_{na}^+ \cdot \mathbf{S}_0^+$. Here, $\mathbf{S}_0^{\pm}$ and $\mathbf{S}_{na}^{\pm}$ represent the entrance (exit) channel free asymptotic and the state-coupling dynamics, respectively, while $\mathbf{S}_b$ is the uncoupled propagation along a series of QBS barriers near the TS. The energies (E_n), widths (Γ_n), and wave functions (ϕ_n^{QBS}) of the QBS can be extracted from the quantum dynamics [20,21] or can be obtained approximately [22]. This information is sufficient to construct the diagonal barrier crossing term, $\mathbf{S}_b$, which has been plotted in Fig. 2(a). The coupling matrices, $\mathbf{S}_{na}^{\pm}$, are represented using a Franck-Condon (FC) type model [23]. This model assumes that the incoming reagents instantaneously transform into a sum of QBS, and likewise the QBS instantaneously decay to products. For the rotor → bend evolution along the reaction coordinate, which is the key to the rotational state distribution, this FC picture is consistent with the actual time scale separation of the dynamics. Thus, the coupling matrices are FC-factors, $\langle \phi_n^{\mathrm{QBS}} | \Psi_0 \rangle$, and the state-specific reaction probabilities are written as

$$P_R(i \to f) = \left| \sum_n \langle \Psi_0(f) | \phi_n^{\mathrm{QBS}} \rangle S_{n,n}^b \langle \phi_n^{\mathrm{QBS}} | \Psi_0(i) \rangle \right|^2 = \left| \sum_n \frac{\langle \Psi_0(f) | \phi_n^{\mathrm{QBS}} \rangle \langle \phi_n^{\mathrm{QBS}} | \Psi_0(i) \rangle}{\sqrt{1 + e^{\Delta E_n / 2\Gamma_n}}} \right|^2 .$$

The free states, Ψ_0, are projected unto the QBS using the FC prescription while the barrier crossing dynamics is modeled with the parabolic model. The overlaps are computed in the TS-dividing plane where the reaction coordinate is fixed. For simplicity, the QBS wave functions are determined by diagonalizing $\boldsymbol{H}$ on the TS-dividing surface. As shown in Fig. 3, the FC model provides a good model of the exact P_R.

To obtain the DCS, we need to combine the amplitudes for different values of the total angular momentum J. As discussed previously [10,12], however, this impact parameter averaging is minimized for backward scattering that tends to strongly resemble the results for low J. Thus, the product distribution predicted by the simple FC model

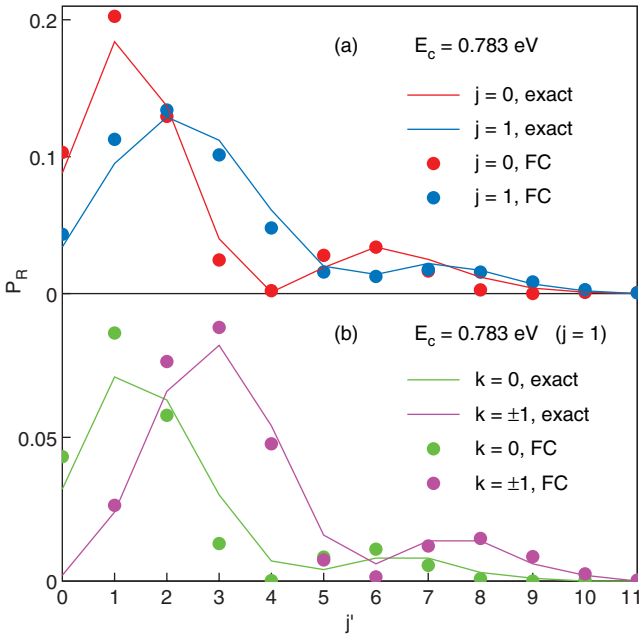

FIG. 3 (color). A comparison of the model prediction to the results of exact quantum scattering calculations for product distribution. In (a), the model is seen to reproduce the differences between p-H_2 and o-H_2 reagent at $E_C = 0.786$ eV. (b) Illustrates the differences between the distribution from $k = 0$ and $k = \pm 1$ states that pass through different QBS pathways.

computed for a single average J (here, 1 and 3) is shown in Fig. 1, and is seen to reproduce the experimental results.

We can now explain the unusual differences between the product quantum state distributions of the p-H_2 and o-H_2 scatterings shown in Fig. 1. At low E_C, the $D + p$-H_2 the reaction is dominated by the lowest QBS, $(0, 0^0)$, that opens at $E_C = 0.35$ eV. The rotational product distribution is unimodal and peaked at $j' = 2$ and consistent with the formation and decay of a single QBS. The next significant QBS contributing to the p-H_2 reaction is the $(0, 2^0)$ state that opens at $E_C = 0.62$ eV. This bend-excited QBS leads to a second peak in the product distribution centered near $j' = 7$. The beam of o-H_2 is composed of two distinct reagent types that combine incoherently to yield the observed DCS. The $k = 0$ component behaves the same as the p-H_2. But, as E_C passes the state energy for the $(0, 1^1)$, the contribution from $k = \pm 1$ rapidly switches on. As shown in Fig. 2(c), the ratio of the total DCS for backward scattering of o-H_2:p-H_2 then exhibits step structure versus E_C as bottleneck energy is passed. The experimental results obtained are seen to be completely consistent with theory. At $E_C = 0.315$ eV, where reactive tunneling dominates, the intensity of o-H_2 scattering (that is solely mediated by the cartwheel state) outstrips that of p-H_2 because the extra 15 meV of rotational energy promotes the tunneling rate. In Fig. 2(c), we see that the opening of the odd bottleneck states $(0, 1^1)$ and $(1, 1^1)$ give rise to discernible features in the DCS ratio since these states mediate the reactivity of the helicopter reagent states. Finally, we note that the differences in the product distributions between p-H_2 and o-H_2 reagent are also explained in terms of this picture. At $E_C = 0.315$ eV, only the o-$H_2(k = 0)$ state is reactive and it passes through the $(0, 0^0)$ QBS. Therefore, aside from the overall intensity that is explained by the tunneling factors in S_b, the product distribution is the same as for p-H_2. At $E_C = 0.783$ eV, the odd-Λ QBS contribute to the signal. As shown in Fig. 3, the bimodal j' distribution for o-H_2 is suppressed since the $k = 0, \pm 1$ contributions peak at different j' values.

In summary, we have demonstrated that product quantum state distribution of the direct chemical reaction $D + H_2$ is determined largely by the dynamics at the TS. The effect of reagent rotation is understood from the orientation of the incoming diatom that is strongly correlated to the vibrational-angular momentum of the QBS, thus providing a unique stereodynamical control of transition-state pathways in a direct chemical reaction.

This work was supported by the NSC and AS of Taiwan, and from the CAS and the MOST of China.

*Electronic address: xmyang@dicp.ac.cn
Electronic address: skodje@spot.colorado.edu

[1] N. Sathyamurthy, Chem. Rev. **83**, 601 (1983).
[2] J. C. Polanyi and W. L. Wong, J. Chem. Phys. **51**, 1439 (1969).
[3] J. M. Bowman, Int. J. Quantum Chem. Quantum Biol. Symp. **30**, 681 (1986).
[4] D. C. Clary, J. Phys. Chem. **99**, 13 664 (1995).
[5] R. Schinke, R. L. Van der Wal, J. L. Scott, and F. F. Crim, J. Chem. Phys. **94**, 283 (1991).
[6] U. Peskin, W. H. Miller, and H. Reisler, J. Chem. Phys. **102**, 8874 (1995).
[7] D. C. Chatfield, R. S. Friedman, D. C. Schwenke, and D. G. Truhlar, J. Phys. Chem. **96**, 2414 (1992).
[8] D. C. Chatfield, R. S. Friedman, D. G. Truhlar, and D. W. Schwenke, Faraday Discuss. Chem. Soc. **91**, 289 (1991).
[9] T. Seideman and W. H. Miller, J. Chem. Phys. **95**, 1768 (1991).
[10] S. A. Harich, D. Dai, C. C. Wang, X. Yang, S. D. Chao, and R. T. Skodje, Nature (London) **419**, 281 (2002).
[11] S. C. Althorpe *et al.*, Nature (London) **416**, 67 (2002).
[12] D. Dai, C. C. Wang, S. A. Harich, X. Yang, S. D. Chao, and R. T. Skodje, Science **300**, 1730 (2003).
[13] R. T. Skodje and X. Yang, Int. Rev. Phys. Chem. **23**, 253 (2004).
[14] L. Schnieder *et al.*, Science **269**, 207 (1995).
[15] M. Zhao, D. G. Truhlar, D. W. Schwenke, and D. J. Kouri, J. Phys. Chem. **94**, 7074 (1990).
[16] A. I. Boothroyd, W. J. Keogh, P. G. Martin, and M. R. Peterson, J. Chem. Phys. **104**, 7139 (1996).
[17] D. M. Skouteris, J. F. Castillo, and D. E. Manolopolous, Comput. Phys. Commun. **133**, 128 (2000).
[18] S. D. Chao and R. T. Skodje, Chem. Phys. Lett. **336**, 364 (2001).
[19] G. C. Schatz and A. Kuppermann, J. Chem. Phys. **65**, 4668 (1976).
[20] R. Sadeghi and R. T. Skodje, J. Chem. Phys. **102**, 193 (1995).
[21] R. T. Skodje, R. Sadeghi, H. Koppel, and J. L. Krause, J. Chem. Phys. **101**, 1725 (1994).
[22] D. G. Truhlar, B. C. Garrett, and S. J. Klippenstein, J. Phys. Chem. **100**, 12 771 (1996).
[23] G. C. Schatz and J. R. Ross, J. Chem. Phys. **66**, 1037 (1977).